

Thermal Behavior of the Antiferromagnet $\text{MnBr}_2 \cdot 4\text{H}_2\text{O}$ in Applied Magnetic Fields*

J. H. SCHELLENG† AND S. A. FRIEDBERG
Carnegie-Mellon University, Pittsburgh, Pennsylvania 15213
 (Received 6 March 1969)

The heat capacity C_p of a single-crystal specimen of $\text{MnBr}_2 \cdot 4\text{H}_2\text{O}$ has been measured between 1.4[°] and 8°K with magnetic fields from 0 to 15 kOe applied along the c' axis. This axis, which is orthogonal to the a and b axes of this monoclinic substance, is thought to be close to the direction of preferred spin orientation in the antiferromagnetic state [$T_N(H=0) = 2.13^\circ\text{K}$]. Temperature changes associated with adiabatic magnetization (magnetocaloric effect) have also been observed. For $H \geq 0$, C_p exhibits at $T_N(H)$ a λ anomaly whose maximum shifts to lower temperature with increasing H , tracing out in the H - T plane a portion of the boundary between antiferromagnetic and paramagnetic phases. Isentropic lines originating within the antiferromagnetic region of this diagram show cooling with initial increase of H , appear to intersect the phase boundary at their inflection points with common tangent, and exhibit temperature minima in the paramagnetic region. The phase boundary is nearly parabolic, with the same curvature as is deduced thermodynamically from zero-field susceptibility and heat-capacity data.

INTRODUCTION

THE antiferromagnets $\text{MnCl}_2 \cdot 4\text{H}_2\text{O}$ ($T_N \approx 1.6^\circ\text{K}$) and $\text{MnBr}_2 \cdot 4\text{H}_2\text{O}$ ($T_N \approx 2.1^\circ\text{K}$) are convenient materials in which to study the effects of relatively large applied magnetic fields on phase transitions within a system of coupled spins. Because of their low Néel points and the large moment of the Mn^{++} ion ($S = \frac{5}{2}$), the effective molecular fields representing the coupling of ionic moments are comparable in magnitude with fields produced by conventional laboratory electromagnets.¹

The behavior of an antiferromagnet in a large external field has been treated theoretically with the help of various microscopic models.^{2,3} A familiar prediction of these calculations is that the Néel point $T_N(H)$ shifts to lower temperatures with increasing field, tracing out in the H - T plane a boundary curve separating antiferromagnetic and paramagnetic phases. When anisotropy is taken into account explicitly, the details of this phase diagram are found to depend on the relative magnitudes of the exchange and anisotropy energies as well as the orientation of the applied field with respect to the preferred direction of spin alignment. For an antiferromagnet with comparatively small anisotropy and the applied magnetic field parallel to the preferred direction, the antiferromagnetic region of the phase diagram is itself subdivided by the so-called "spin-flop"

boundary. This situation is illustrated schematically in Fig. 1. The spin-flop boundary may be crossed by increasing the applied field isothermally at a sufficiently low temperature ($T < T_3$). The resulting transition is characterized by the abrupt switching of the antiferromagnetically coupled spins to an orientation perpendicular to that of the applied field. Further raising of the field eventually produces another abrupt but less dramatic transition as the system passes into the paramagnetic phase.

A phase diagram exhibiting these three regions has been constructed in some detail for single-crystal $\text{MnCl}_2 \cdot 4\text{H}_2\text{O}$ from observations of the magnetization,⁴ proton^{4,5} and antiferromagnetic resonance,^{4,6,7} optical Zeeman effect,⁸ and susceptibility.⁹ In this paper, we shall be concerned with $\text{MnBr}_2 \cdot 4\text{H}_2\text{O}$, whose phase diagram has not been fully explored in spite of its more accessible Néel temperature. Previously,¹⁰ we reported

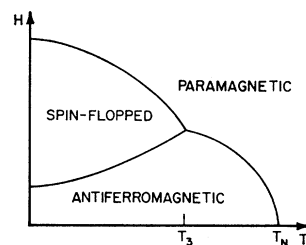


FIG. 1. Schematic phase diagram for an antiferromagnet with weak anisotropy in a magnetic field applied along the preferred direction of spin alignment.

* Work supported by the Office of Naval Research and the National Science Foundation. Based on part of a thesis submitted by J. H. Schelling to the Carnegie-Mellon University in partial fulfillment of the requirements for the Ph.D. degree. Preliminary accounts of some of these results have appeared in *Bull. Am. Phys. Soc.* **8**, 212 (1963), and in *Proceedings of the International Conference on Magnetism, Nottingham, 1964* (The Institute of Physics and The Physical Society, London, 1965), p. 90.

† Present address: U. S. Naval Research Laboratory, Washington, D. C.

¹ S. A. Friedberg and J. D. Wasscher, *Physica* **19**, 1072 (1953).
² C. J. Gorter and T. van Peski-Tinbergen, *Physica* **22**, 278 (1956); C. J. Gorter, *Nuovo Cimento* **6**, 5923 (1957).

³ J. Kanamori, K. Motizuki, and K. Yosida, *Busseiron-Kenkyu* **63**, 28 (1953). A summary of this work in English is in the Appendix to *J. Phys. Soc. Japan* **14**, 759 (1959).

⁴ H. M. Gijssman, N. J. Poullis, and J. vanden Handel, *Physica* **25**, 954 (1959).

⁵ R. D. Spence and V. Nagarajan, *Phys. Rev.* **146**, 191 (1966).

⁶ B. Bölger, in *Conférence de Physique des Basses Températures, Paris, 1955* (Centre Nationale de la Recherche Scientifique, and UNESCO, Paris, 1956), p. 244.

⁷ M. Abkowitz and A. Honig, *Phys. Rev.* **136**, A1003 (1964).

⁸ I. Tsujikawa and E. Kanda, *J. Phys. Radium* **20**, 352 (1959); *J. Phys. Soc. Japan* **18**, 1382 (1963).

⁹ J. E. Rives, *Phys. Rev.* **162**, 491 (1967).

¹⁰ J. H. Schelling and S. A. Friedberg, *J. Appl. Phys.* **34**, 1087 (1963).

heat-capacity and magnetocaloric measurements on a powder specimen of this salt. These experiments revealed several anticipated features, including: (a) the shift of the anomaly in C_p to lower temperatures with increasing field; (b) rounding and broadening of the anomaly due to the distribution of angles between the field and preferred spin direction in the polycrystalline specimen and to field inhomogeneity caused by demagnetizing effects; and (c) cooling upon adiabatic magnetization from initial temperatures below $T_N(0)$.

We now wish to report measurements of the heat capacity of a single crystal of $\text{MnBr}_2 \cdot 4\text{H}_2\text{O}$ in applied magnetic fields between 0 and 15 kG at temperatures from 1.4 to 8°K. These data are supplemented by magnetocaloric measurements over the same ranges of field and temperature. One aspect of the latter results is again the observation of cooling of an antiferromagnet by adiabatic magnetization. Theoretical attention^{11,12} given this particular topic has stimulated us to look for the effect in MnF_2 . These results will be summarized briefly.

EXPERIMENTAL DETAILS

These experiments were performed in a vacuum calorimeter whose sample chamber and Dewar assembly were designed to fit in the 2-in. gap of a C-type electromagnet providing fields up to ~ 24 kOe. The vacuum system was unusual in that all seals regularly opened to load or service the apparatus were of the rubber O-ring type and were kept at room temperature.

The $\text{MnBr}_2 \cdot 4\text{H}_2\text{O}$ specimens employed in this investigation were prepared by recrystallization from aqueous solutions of material obtained from the Fielding Chemical Co. Analysis indicates that the dominant impurity in this material was zinc, which was present initially to the extent of < 0.2 wt.%. The specimens contained no more than 0.004-wt.% Fe, 0.002-wt.% Mo, 0.0007-wt.% Cr, and 0.0005-wt.% Cu. No other transition metal impurities were detected spectrographically. Most of the data to be described below were obtained on a roughly spherical specimen having a mass of 7.794 g (0.02718 mole). To prevent its decomposition, this crystal was covered with a thin coating of nylon gauze and lacquer. The necessary calorimetric accessories were attached to a small sheet-copper holder which was lacquered to the crystal. These included a 100- Ω heater winding of 36 Manganin wire and a resistance thermometer consisting of a 0.1-W Allen-Bradley carbon radio resistor with a nominal value of 57 Ω . During each experiment the thermometer was calibrated against the vapor pressure of the cryogenic liquid bath at several temperatures, a hydrostatic head correction being applied where appropriate. Vapor pressures were reduced to temperature in terms

of the 1958 He⁴ scale¹³ and the National Bureau of Standards data¹⁴ for equilibrium liquid hydrogen. Thermal contact between specimen and refrigerant during calibration was achieved by introducing a small amount of helium gas into the vacuum chamber.

Heat capacities were measured by the conventional method of discontinuous heating. The small heat capacity of the single-crystal accessories was found by comparison of the single-crystal and powder results¹⁰ in zero applied field.

Adiabatic magnetization measurements were carried out in discrete steps. Starting at zero external field and initial temperatures either above or below $T_N(0)$, the field was slowly increased until a given value was reached. Upon attainment of equilibrium, the specimen temperature was noted and the field again increased. After a series of such steps had brought the field to its maximum value, the process was reversed, the rate of change of the magnetic field being kept of fixed magnitude. In most cases the only irreversible effect was a slight eddy-current heating of the metal parts of the sample assembly. By combining magnetization and demagnetization data, a correction could be made for this effect.

RESULTS AND DISCUSSION

Figure 2 shows the results of heat-capacity measurements on a single crystal of $\text{MnBr}_2 \cdot 4\text{H}_2\text{O}$ in applied fields H_a of 0, 5.06, 8.30, 10.01, and 15.00 kOe. The specimen was mounted so that H_a was parallel to the c' axis which is orthogonal to both a and b axes of this monoclinic structure ($\beta = 99^\circ 6'$).¹⁵ It lies in the a - c plane and makes an angle of $9^\circ 6'$ with the c axis. This orientation was chosen because of optical evidence⁸ of spin flopping produced by a magnetic field applied along the c' axis. The c axis had originally been assumed⁴ to be the preferred direction in the ordered state as it is in $\text{MnCl}_2 \cdot 4\text{H}_2\text{O}$. However, since magnetic observations⁴ with $H \parallel c$ had not revealed spin flopping above 1°K, it appeared likely that the c' axis was closer to the preferred direction. Recent magnetization data¹⁶ are consistent with this idea, although, as we shall see below, it is still not clear precisely where the preferred direction lies or how accurately the field and specimen must be aligned to permit the observation of spin flopping in this salt if, in fact, it does occur above 1°K. Specimen alignment was accomplished using the data of Groth¹⁵ and verified by x-ray back-reflection photography. Alignment in the cryostat was believed to be accurate to within about $\pm 2^\circ$.

The data for $H_a = 0$ agree well with the powder data

¹³ H. van Dijk, M. Durieux, J. R. Clement, and J. K. Logan, Natl. Bur. Std. (U. S.) Monograph 10, (1960).

¹⁴ H. Woolley, R. B. Scott, and F. G. Brickwedde, J. Res. Natl. Bur. Std. (U. S.) 41, 379 (1948).

¹⁵ P. Groth, *Chemische Kristallographie* (Engelmann, Leipzig, 1906), Vol. 1 p. 245.

¹⁶ V. A. Schmidt and S. A. Friedberg, J. Appl. Phys. 38, 5319 (1967).

¹¹ E. A. Turov, Zh. Eksperim. i Teor. Fiz. 34, 1009 (1958) [English transl.: Soviet Phys.—JETP 8, 696 (1958)].

¹² R. Joenk, Phys. Rev. 128, 1634 (1962).

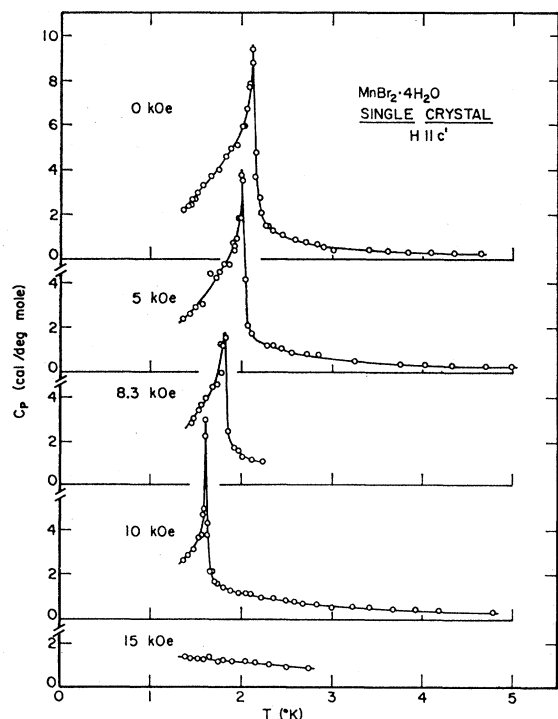


FIG. 2. Heat capacity of a single crystal of $\text{MnBr}_2 \cdot 4\text{H}_2\text{O}$ as a function of temperature for several values of magnetic field applied along the c' axis. The same vertical scale applies to each curve with the zero displaced as shown.

of Kapadnis and Hartmans¹⁷ as well as our own.¹⁰ The latter results were obtained on a 12.886-g (0.04493-mole) sample of the same material employed in this work. Since they have been reported¹⁰ only in graphical form, we list them in Table I together with the zero-field single-crystal C_p values. In both cases the anomalous maximum locates the Néel point $T_N(0)$ at $(2.13 \pm 0.01)^\circ\text{K}$.

The most striking feature of these results seen in Fig. 2 is the fact that the specific-heat anomaly in non-zero applied magnetic fields retains the sharp λ character it has for $H_a = 0$, at least to the resolution of our experiments ($\Delta T \approx 10^{-2}^\circ\text{K}$ at T_N). As expected, depression of the peak temperature for given applied field H_a is larger than that seen for a powder specimen. For $H_a = 15.0$ kOe, the peak, and thus $T_N(H)$, is already shifted below the range of our measurements.

The portion of the antiferromagnetic-paramagnetic phase boundary corresponding to the locus of these maxima is shown in Fig. 3. Here, H_a at the transition has been plotted against transition temperature. For purposes of comparison with theory, it may be necessary to correct these fields to the values appropriate to an infinitely long needlelike specimen, the internal fields H_i . This may be done using the magnetization data of Schmidt and Friedberg¹⁶ and the relation $H_i = H_a - DM$, where, in this case, the demagnetizing factor D

is roughly that of a sphere. The open squares in Fig. 3 indicate the corrected transition points.

From our zero-field measurements on powdered $\text{MnBr}_2 \cdot 4\text{H}_2\text{O}$, we concluded that, between 6 and 14°K , the heat capacity could be represented as a sum of where lattice and magnetic parts, namely, $C_p/R = aT^3 + bT^{-2}$, where $a = 2.8 \times 10^{-4} (\text{Kdeg})^{-3}$ and $b = 2.24 (\text{Kdeg})^2$. Assuming the same lattice term to be valid below 6°K and to be unaffected by applied magnetic fields, we have separated out the magnetic contribution to C_p for each set of single-crystal data. Evaluating $\Delta S_{\text{mag}} = \int_{1.4}^T (C_{\text{mag}}/T) dT$, curves of magnetic entropy versus temperature have been constructed for each value of H_a . As before,¹⁰ the positions of these curves relative to

TABLE I. Heat capacity of $\text{MnBr}_2 \cdot 4\text{H}_2\text{O}$ without applied field. C_p in cal/mole deg. Temperature in $^\circ\text{K}$.

| A. Powdered specimen (0.04495 mole) | | | | | |
|-------------------------------------------|--------|-------|--------|--------|--------|
| T | C_p | T | C_p | T | C_p |
| 1.373 | 2.366 | 2.445 | 0.9919 | 10.178 | 0.608 |
| 1.454 | 2.631 | 2.537 | 0.8648 | 10.178 | 0.579 |
| 1.533 | 2.575 | 2.786 | 0.6542 | 10.468 | 0.579 |
| 1.604 | 3.261 | 2.908 | 0.5827 | 10.600 | 0.684 |
| 1.694 | 3.717 | 3.021 | 0.5324 | 10.766 | 0.751 |
| 1.805 | 4.353 | 3.139 | 0.4857 | 10.844 | 0.756 |
| 1.918 | 5.253 | 3.255 | 0.4447 | 10.987 | 0.705 |
| 2.012 | 6.343 | 3.367 | 0.4123 | 11.264 | 0.781 |
| 2.026 | 6.519 | 3.470 | 0.3835 | 11.398 | 0.812 |
| 2.041 | 8.669 | 3.582 | 0.3581 | 11.573 | 0.827 |
| 2.045 | 6.831 | 3.937 | 0.2973 | 11.864 | 0.949 |
| 2.063 | 7.325 | 4.117 | 0.2382 | 11.888 | 0.991 |
| 2.071 | 7.627 | 4.289 | 0.2460 | 12.317 | 1.102 |
| 2.084 | 7.975 | 4.477 | 0.2297 | 12.699 | 1.181 |
| 2.090 | 7.937 | 4.660 | 0.2163 | 13.048 | 1.303 |
| 2.096 | 8.745 | 4.871 | 0.2030 | 13.451 | 1.296 |
| 2.105 | 9.633 | 5.047 | 0.1972 | 13.864 | 1.712 |
| 2.114 | 10.464 | 5.187 | 0.1921 | 14.209 | 1.501 |
| 2.119 | 10.380 | 5.390 | 0.1814 | 14.580 | 1.776 |
| 2.131 | 3.179 | 5.676 | 0.1840 | 14.901 | 1.99 |
| 2.142 | 3.251 | 5.925 | 0.1854 | 15.284 | 2.04 |
| 2.152 | 2.443 | 6.269 | 0.190 | 15.807 | 2.26 |
| 2.179 | 1.958 | 6.688 | 0.198 | 16.328 | 2.62 |
| 2.187 | 1.896 | 7.065 | 0.219 | 16.788 | 2.52 |
| 2.234 | 1.560 | 7.482 | 0.246 | 17.278 | 2.85 |
| 2.242 | 1.519 | 7.920 | 0.286 | 17.462 | 2.61 |
| 2.309 | 1.264 | 8.432 | 0.376 | 18.219 | 3.37 |
| 2.319 | 1.2603 | 8.971 | 0.413 | 18.783 | 2.72 |
| 2.331 | 1.2111 | 9.423 | 0.488 | 19.364 | 3.23 |
| 2.439 | 0.9950 | 9.826 | 0.515 | 19.978 | 3.50 |
| B. Single-crystal specimen (0.02718 mole) | | | | | |
| T | C_p | T | C_p | T | C_p |
| 1.352 | 2.1857 | 2.083 | 7.7419 | 3.009 | 0.4776 |
| 1.397 | 2.3114 | 2.108 | 8.7718 | 3.243 | 0.6313 |
| 1.434 | 2.4192 | 2.131 | 9.4026 | 3.407 | 0.4092 |
| 1.450 | 2.6501 | 2.142 | 3.3535 | 3.614 | 0.3589 |
| 1.476 | 2.6479 | 2.154 | 4.8054 | 3.838 | 0.3182 |
| 1.503 | 2.9258 | 2.200 | 2.0071 | 4.078 | 0.2812 |
| 1.570 | 3.1943 | 2.201 | 2.7641 | 4.338 | 0.2506 |
| 1.611 | 4.9441 | 2.267 | 1.5017 | 4.639 | 0.2264 |
| 1.669 | 3.6187 | 2.271 | 1.4956 | 5.332 | 0.1190 |
| 1.762 | 3.9701 | 2.339 | 1.2851 | 5.582 | 0.1152 |
| 2.002 | 5.9055 | 2.447 | 1.0484 | 6.203 | 0.1880 |
| 2.026 | 5.9043 | 2.583 | 0.8754 | 6.654 | 0.2007 |
| 2.055 | 6.7481 | 2.715 | 0.7374 | 7.024 | 0.2133 |
| 2.060 | 7.0381 | 2.824 | 0.6489 | 7.398 | 0.2372 |
| 2.082 | 7.9069 | 2.921 | 0.5735 | 7.800 | 0.2533 |

¹⁷ D. G. Kapadnis and R. Hartmans, *Physica* **22**, 181 (1956).

that for $H=0$ have been fixed by magnetocaloric experiments. One notes simply that adiabatic magnetization to the field in question from $H=0$ determines a point through which the entropy-temperature curve for that field must pass. A plausible extrapolation of the corrected C_p data for $H=0$ to 0°K permits the establishment of a zero of magnetic entropy reliable to within about 2%. The results are shown in Fig. 4. Since the lattice entropy at 4°K amounts to about 4×10^{-3} cal/deg mole, Fig. 4 is nearly equivalent to a diagram of the total entropy.

We note in Fig. 4 that all the entropy curves for $H_a > 0$ cross the curve for $H_a = 0$. Thus, for $T < T_N(0)$, the entropy of an antiferromagnet increases upon isothermal magnetization (vertical displacement in Fig. 4) at least until the system is forced into the paramagnetic phase. Correspondingly, adiabatic magnetization (horizontal displacement in Fig. 4) from an initial temperature $T_i < T_N(0)$ produces cooling while the material is in the antiferromagnetic phase. The possibility of achieving cooling by this process appears to have been first recognized by Kurti¹⁸ in a study of systems becoming antiferromagnetic well below 1°K . As one would anticipate, the cooling accompanying a given adiabatic field increase from the same initial temperature, $T_i < T_N(0)$, is greater for the single-crystal specimen with parallel field orientation than was observed for a powder specimen. The observed cooling agrees well with that calculated with the usual thermodynamic expression for the magnetocaloric effect using measured values of the temperature coefficient of magnetization and the heat capacity.

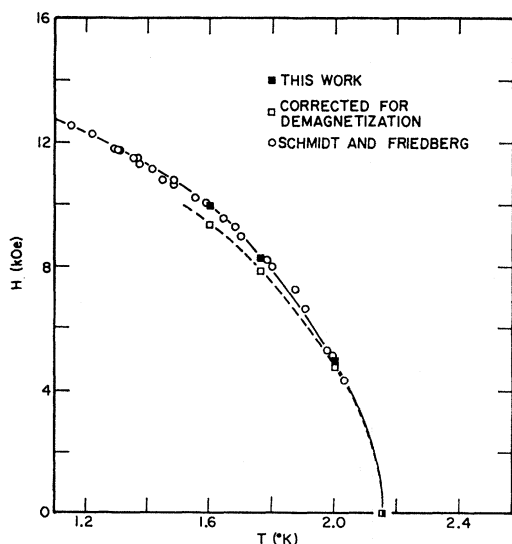


FIG. 3. Portion of the phase diagram for $\text{MnBr}_2 \cdot 4\text{H}_2\text{O}$ with $H \parallel c'$. Solid squares give the positions of the maxima of the heat-capacity curves of Fig. 2. The open squares represent these points after correction of the field to H_{int} . The dashed curve is a parabola as described in the text.

¹⁸ N. Kurti, J. Phys. Radium **12**, 281 (1951); A. J. P. Meyer, Compt. Rend. **248**, 202 (1959).

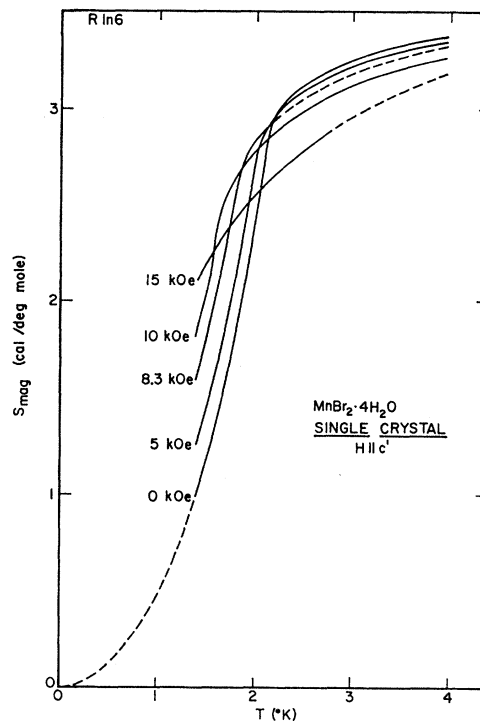


FIG. 4. Entropy of a single crystal of $\text{MnBr}_2 \cdot 4\text{H}_2\text{O}$ as a function of temperature for several values of applied field.

A proper microscopic calculation of the magnetocaloric effect in an antiferromagnet is practical at sufficiently low temperatures where the spin-wave¹¹ approximation is valid. Such a calculation would probably not be useful in the present case because the data have been obtained rather close to $T_N(0)$. However, Joenk¹² has used a spin-wave model of MnF_2 ($T_N = 67^\circ\text{K}$) to predict the magnetocaloric cooling of that salt. We have verified these predictions in fields up to 20 kOe at temperatures below 4°K . These results are summarized in Appendix A.

In Fig. 5 the results of magnetocaloric measurements from several initial temperatures above and below $T_N(0)$ are displayed by plotting experimental isentropic curves on a diagram of H_a versus T . The dashed curve in this figure is the locus of $C_{p,H}$ maxima, i.e., the empirical phase boundary. Some details of this diagram will be discussed below. We should mention at this point, however, that one of our primary reasons for obtaining isentropic curves was the hope that we might detect spin flopping rather directly by this means. If, as theory suggests,^{2,3} the spin-flop transition is of first order and accompanied by the release of a quantity of latent heat, one might expect a temperature jog in the isentrope as the phase boundary is crossed with increasing field. One series of magnetocaloric observations not shown in Fig. 5 apparently gave evidence of abrupt energy release with hysteresis, suggesting the occurrence of a first-order phase change. This effect seemed to appear for values of H_a and T near which spin

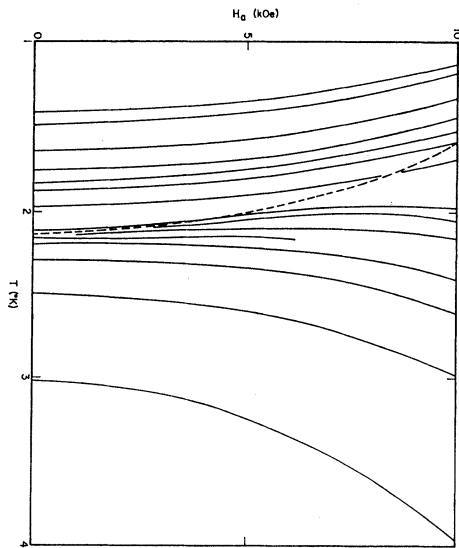


Fig. 5. Results of adiabatic magnetization experiments on single-crystal $\text{MnBr}_2 \cdot 4\text{H}_2\text{O}$ with $\mathbf{H}_a \parallel c'$. The solid lines are isentropic curves. The dashed line represents the empirical antiferromagnetic-paramagnetic phase boundary.

flopping had been inferred from other work.^{6,8} However, we were unable to reproduce the effect after remounting the specimen and cannot conclude that spin flopping has been confirmed in $\text{MnBr}_2 \cdot 4\text{H}_2\text{O}$, at least with $\mathbf{H}_a \parallel c'$ axis. Subsequent isothermal magnetization¹⁶ studies give no evidence of spin flopping above 1.15°K with $\mathbf{H}_a \parallel c'$ or with $\mathbf{H}_a \parallel c$, in agreement with the original findings of Gijsman *et al.*⁴

It is possible, of course, that the range of angles between the applied field and preferred spin direction within which spin flopping is readily detectable may be quite small in $\text{MnBr}_2 \cdot 4\text{H}_2\text{O}$. If this were so and neither the c' nor the c axis was close enough to the preferred direction or if misalignment of the specimen were too great in one or more of the experiments to date, it would be possible to reconcile the conflicting indications for and against spin flopping in the salt. Unfortunately, in none of these experiments, including our own, has it been practical to rotate the specimen *in situ* and establish precisely the preferred axis by detection of an extremum in a measured property. This is clearly very desirable and magnetization measurements to this end are being undertaken.

Evidently, we are concerned in this work only with antiferromagnetic-paramagnetic phase transitions. From the appearance of the heat-capacity anomalies in Fig. 2, it seems likely that these are of the λ type and not simple second-order transitions as predicted by molecular-field theory. The thermodynamic theory of λ transitions^{19,20} provides a basis for correlating and interpreting a number of observations in $\text{MnBr}_2 \cdot 4\text{H}_2\text{O}$.

¹⁹ M. J. Buckingham and W. M. Fairbank, in *Progress in Low-Temperature Physics*, edited by C. J. Gorter (North-Holland Publishing Co., Amsterdam, 1961), Vol. 3, p. 80.

²⁰ A. B. Pippard, *Elements of Classical Thermodynamics* (Cambridge University Press, New York, 1957), p. 143.

One consequence of the theory, adapted to magnetic state variables, is the relation²¹

$$\frac{C_H}{T} = \left(\frac{dH}{dT_N} \right)^2 \left(\frac{\partial M}{\partial H} \right)_T + K, \quad (1)$$

where dH/dT_N is the slope of the phase boundary, $(\partial M/\partial H)_T$ is the differential isothermal susceptibility, and K is a group of terms which, though large near T_N , do not vary rapidly with T for certain classes of systems. Assuming the λ anomalies in $\text{MnBr}_2 \cdot 2\text{H}_2\text{O}$ to constitute (near) singularities in C_H , Eq. (1), if applicable, predicts for $H=0$ an infinite initial slope of the phase boundary in the absence of any singularity in $(\partial M/\partial H)_T$. This is certainly consistent with the limited data available near $H=0$. For $H>0$, dH/dT_N is clearly finite and a (near) singularity in C_H should be reflected in a corresponding peak in $(\partial M/\partial H)_T$. This has now been observed directly in the magnetization isotherms.¹⁶

Another consequence of the thermodynamic theory is the conclusion that if C_H is (nearly) singular at the transition point, then the phase boundary and any isentrope passing through that point will have the same slope.²² Referring to Fig. 5, we see evidence for such behavior both at $H_a=0$ and for at least two non-zero fields. One of these intersections of an isentrope and the phase boundary is particularly striking in that it appears to coincide with an inflection point of the isentrope. Griffiths²³ has shown that this is just the expected behavior if the heat capacity diverges along the phase boundary as

$$C_H \sim |T - T_N|^{-\alpha} \quad (2)$$

for $\alpha < \frac{1}{2}$. This criterion is satisfied for most model antiferromagnets, including those exhibiting logarithmic singularities in C_H . Recent measurements in zero field suggest that $\text{MnBr}_2 \cdot 4\text{H}_2\text{O}$ also satisfies this requirement.²⁴ Since Griffiths's argument is not generally available, we reproduce it, with his permission, in Appendix B.

Closely associated with the behavior of the isentropes at their intersections with the phase boundary is the fact that they have their extrema at points well within the paramagnetic phase. In other words, adiabatic magnetization continues to cause the antiferromagnet to cool even after it has become nominally paramagnetic. We even see in Fig. 5 one isentrope lying wholly in the paramagnetic region which exhibits a temperature minimum for $H>0$. From the magnetocaloric relation

$$\left(\frac{\partial M}{\partial T} \right)_H = - \frac{C_H}{T} \left(\frac{\partial T}{\partial H} \right)_S, \quad (3)$$

²¹ E. Sawatsky and M. Bloom, *Can. J. Phys.* **42**, 657 (1964).
²² J. Skalyo, Jr., A. F. Cohen, S. A. Friedberg, and R. B. Griffiths, *Phys. Rev.* **164**, 705 (1967).

²³ R. B. Griffiths (private communication).

²⁴ L. Kreps and S. A. Friedberg (unpublished).

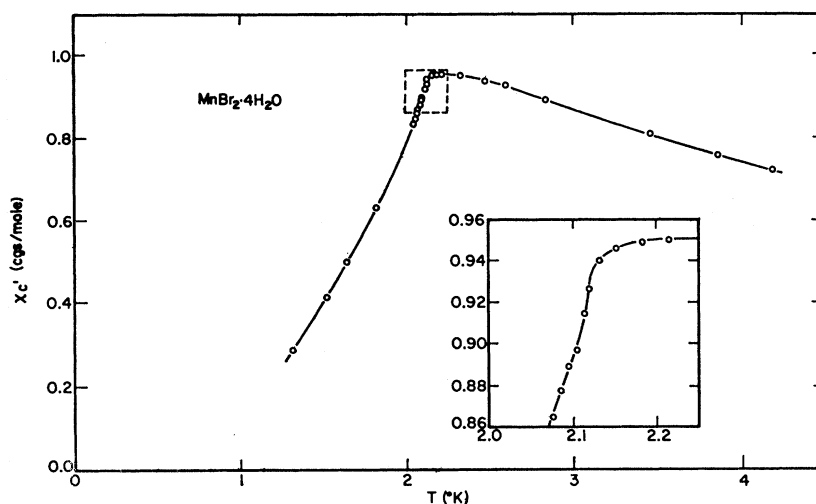


FIG. 6. Magnetic susceptibility of $\text{MnBr}_2 \cdot 4\text{H}_2\text{O}$ along the c' axis as a function of temperature. Measured by Berger at 275 cps.

we infer that at the intersection of isentrope and phase boundary, the (near) singularity in C_H is matched by a (near) singularity in $(\partial M/\partial T)_H$. One also concludes from Eq. (3) that the extremum of the isentrope in the paramagnetic region of the H - T diagram corresponds to $(\partial M/\partial T)_H=0$.

As a further observation on Fig. 5, we note that isentropes close to the phase boundary near $H=0$ may well share not only its initial slope but also its initial curvature. In such a case, Fisher's relation²⁵ between C_H and the susceptibility χ at $H=0$,

$$C_H = A \frac{\partial(\chi T)}{\partial T} = A \frac{\partial \chi}{\partial T} + A\chi, \quad (4)$$

becomes essentially a thermodynamic identity with²²

$$1/A(T_N) = -(\partial^2 T/\partial H^2)_{H=0}. \quad (5)$$

This follows from the differentiation of a Maxwell relation

$$-\left(\frac{\partial^2 T}{\partial H^2}\right)_S = \frac{\partial^2 M}{\partial S \partial H} = \left(\frac{\partial \chi}{\partial S}\right)_H = \left(\frac{\partial \chi}{\partial T}\right)_H \left(\frac{\partial T}{\partial S}\right)_H = \frac{T}{C_H} \left(\frac{\partial \chi}{\partial T}\right)_H \quad (6)$$

and the observation that the term $A\chi$ in Eq. (4) is negligible at the transition temperature $T_N(0)$ in comparison with $A\partial\chi/\partial T$. Since $H=0$, we may interchange adiabatic and isothermal susceptibilities in Eq. (6).

The susceptibility of $\text{MnBr}_2 \cdot 4\text{H}_2\text{O}$ along the c' axis in nearly zero field has been carefully measured through $T_N(0)$ by Berger.²⁶ His results are shown in Fig. 6. A plot of $\chi_{c'} T$ versus $\int_{1.4}^T C_p dT$ yields a straight line, indicating that $\chi_{c'}$ and $C_p(H=0)$ satisfy Fisher's relation. The slope of this line is $A = 8.89 \times 10^7$ Oe²/deg. Let us assume that the phase boundary is parabolic

and thus has the same curvature for $H>0$ as that determined from A at $H=0$. We may represent this parabola as $T_N(H) = T_N(0)(1 - \gamma H^2)$, where $\gamma = \frac{1}{2} \times A T_N(0) = 2.64 \times 10^{-9}$ Oe⁻². A phase boundary calculated in this way is shown in Fig. 3 by the dashed line. It is seen to reproduce rather well the boundary obtained when demagnetizing corrections are applied to the locus of heat-capacity maxima. That the boundary should be so nearly parabolic is consistent with recent calculations by Bienenstock²⁷ for Ising models in large applied parallel fields. His results for the antiferromagnetic-paramagnetic phase boundary are summarized by the formula

$$T_N(H) = T_N(0)[1 - (H/H_C)^2]^\xi,$$

where $\xi = 0.87$, 0.35, and 0.36 for the square, simple cubic, and bcc lattices, respectively. For $H \ll H_C$ this expression reduces to the parabola used above with $\gamma = \xi/H_C^2$. Considering the nearest-neighbor Ising Hamiltonian to be an approximation to the Heisenberg Hamiltonian $-2J \sum_{\langle ij \rangle} \mathbf{S}_i \cdot \mathbf{S}_j$, we may write $H_C = -2S z J / g \mu_B$, where J is the nearest-neighbor exchange integral and z is the number of nearest neighbors to a spin of magnitude S . Taking $S = \frac{5}{2}$, $g = 2.00$, and $\gamma = 2.64 \times 10^{-9}$ Oe⁻², one finds $zJ/k = -0.31$ and -0.49°K for $\xi = 0.35$ and $\xi = 0.87$, respectively.

These numbers may be compared with an estimate obtained from the simple two-sublattice molecular-field model of an antiferromagnet with nearest-neighbor interaction only, which gives $z|J|/k = 3T_N/2S(S+1) = 0.36^\circ\text{K}$. The agreement with the value inferred above for three-dimensional lattices is quite reasonable. A more reliable estimate is obtained from the measured perpendicular susceptibility⁴ for $T < T_N$ by means of a result common to both molecular-field and lowest-order spin-wave theories,²⁸ namely, $z|J|/k = N_0 g^2 \mu_B^2 / 4k\chi_\perp$. Using this relation, one finds $z|J|/k = 0.47^\circ\text{K}$, a value which is closer to that deduced from the fitting of the

²⁷ A. Bienenstock, J. Appl. Phys. **37**, 1459 (1966).

²⁸ T. Nagamiya, H. Yosida, and R. Kubo, Advan. Phys. **4**, 1 (1955).

²⁵ M. E. Fisher, Phil. Mag. **7**, 1731 (1962).

²⁶ L. Berger (private communication).

phase boundary assuming $\xi=0.87$, i.e., a square lattice. It is not obvious from the limited number of cases calculated so far that ξ is determined primarily by dimensionality, nor is it clear how realistic it is in this case to allow only for nearest-neighbor interactions in an Ising approximation. We conclude only that the strength of this interaction deduced from a fit of the antiferromagnetic-paramagnetic phase boundary is of reasonable magnitude and agrees satisfactorily with estimates based on other observations. This agreement extends to additional estimates of nearest-neighbor exchange coupling in $\text{MnBr}_2 \cdot 4\text{H}_2\text{O}$ deduced from other data by Miedema *et al.*²⁹ assuming $z \approx 6$.

ACKNOWLEDGMENTS

We are grateful to Professor R. B. Griffiths and Professor T. Oguchi for several helpful discussions of various aspects of this work. We wish to thank Professor R. B. Griffiths and Professor L. Berger for permission to quote in detail from their unpublished work.

APPENDIX A: SOME MAGNETOCALORIC OBSERVATIONS ON MnF_2

Several series of adiabatic magnetization experiments in fields up to 20 kOe were performed below 4°K on a single crystal of MnF_2 of mass 16.354 g (0.180 mole). The field was applied along the c axis, which is the preferred direction of spin alignment in the antiferromagnetic state ($T_N=67^\circ\text{K}$). Temperature changes were measured with a carbon resistor in a small copper holder lacquered to the crystal. The cooling expected in these fields is much smaller than that observed in $\text{MnBr}_2 \cdot 4\text{H}_2\text{O}$ closer to $T_N(0)$. In spite of the relatively large scatter of the data, we have detected cooling of the predicted magnitude. For example, at an initial temperature $T_i=4.00^\circ\text{K}$ a field increment $\Delta H=20$ kOe produced a fractional temperature change $\Delta T/T_i = -0.012 \pm 0.0001$, which is essentially the value calculated by Joenk.¹² At $T_i=2.155^\circ\text{K}$ the same ΔH yielded $\Delta T/T_i = -0.001 \pm 0.001$, the calculated value being $\Delta T_i/T \approx -0.0018$.

APPENDIX B

We consider an antiferromagnet whose heat capacity at constant magnetic field C_H diverges as the phase boundary separating antiferromagnetic and paramagnetic phases is approached from either the high- or low-temperature side. In Ref. 22 it is shown that for such a system the isentropes are tangent to the phase boundary at the point where they cross the latter. Griffiths has given the following argument to show that if the divergence in C_H is not too rapid, the crossing point is also a point of inflection of the isentrope where $(\partial T/\partial H)_S$ achieves a (local) minimum, and the second derivative diverges to $+\infty$ and $-\infty$ on opposite sides

²⁹ A. R. Miedema, R. F. Wielinga, and J. Huiskamp, *Physica* 31, 835 (1965).

of the phase boundary. In analogy with the work of Buckingham and Fairbank¹⁹ we introduce a new variable

$$s = S - S_b(H), \quad (\text{B1})$$

where $S_b(H)$ is the entropy on the phase boundary. The following relations hold:

$$\left(\frac{\partial S}{\partial H}\right)_s = -\left(\frac{\partial s}{\partial H}\right)_s = -S_b'(H), \quad (\text{B2})$$

$$\left(\frac{\partial}{\partial s}\right)_H = \left(\frac{\partial}{\partial S}\right)_H, \quad (\text{B3})$$

$$\left(\frac{\partial}{\partial H}\right)_s = \left(\frac{\partial}{\partial H}\right)_s - S_b'(H) \left(\frac{\partial}{\partial S}\right)_H. \quad (\text{B4})$$

Applying (B4) to the temperature yields

$$\left(\frac{\partial T}{\partial H}\right)_s = \left(\frac{\partial T}{\partial H}\right)_s + S_b'(H) \left(\frac{\partial T}{\partial S}\right)_H. \quad (\text{B5})$$

Applying (B4) to (B5) and using (B2) and (B3) to rewrite some of the terms, one obtains

$$\begin{aligned} \left(\frac{\partial^2 T}{\partial H^2}\right)_s &= \left(\frac{\partial^2 T}{\partial H^2}\right)_s - S_b''(H) \left(\frac{\partial T}{\partial S}\right)_H \\ &\quad - 2S_b'(H) \left[\frac{\partial}{\partial H} \left(\frac{\partial T}{\partial S}\right)_H \right]_s + [S_b'(H)]^2 \left(\frac{\partial^2 T}{\partial S^2}\right). \end{aligned} \quad (\text{B6})$$

Near the phase boundary, the first term on the right-hand side of (B6) approaches the curvature of the boundary, and the next two terms, proportional to $1/C_H$ and its derivative along the boundary, become very small by our basic assumption. The last term, which may be written

$$-[S_b'(H)]^2 \frac{(\partial^2 S/\partial T^2)_H}{(\partial S/\partial T)_H^3} \quad (\text{B7})$$

depends critically on the manner in which C_H diverges. Thus, if C_H (for fixed H) diverges as

$$C_H \sim |T - T_b|^{-\alpha}, \quad (\text{B8})$$

where T_b is the temperature of the phase boundary, (B7) is proportional to

$$|T - T_b|^{2\alpha-1} \text{sgn}(T - T_b). \quad (\text{B9})$$

For $\alpha < \frac{1}{2}$ (and also for a logarithmic divergence of C_H), (B7) diverges to $+\infty$ for $T > T_b$ and $-\infty$ for $T < T_b$. Thus, the crossing point of the phase boundary and isentrope occurs at an inflection point of the latter. This situation appears to be realized in $\text{MnBr}_2 \cdot 4\text{H}_2\text{O}$, at least over the portion of phase boundary we have examined. Note that for $\alpha > \frac{1}{2}$, (B7) goes to zero and by (B6) the curvatures of the isentrope and the phase boundary coincide at the crossing point. Griffiths has observed that, since the isentrope and phase boundary coincide over a finite interval in a first-order transition, the case $\alpha > \frac{1}{2}$ may be regarded as an "incipient" first-order phase change.